

A study of the strong pulses detected from PSR B0656+14 using the Urumqi 25-m radio telescope at 1540 MHz *

Guo-Cun Tao^{1,2}, Ali Esamdin¹, Hui-Dong Hu^{1,2}, Mao-Fei Qian^{1,2}, Jing Li^{1,2} and Na Wang¹

¹ Xinjiang Astronomical Observatory, Chinese Academy of Sciences, Urumqi 830011, China; aliyi@xao.ac.cn

² Graduate University of Chinese Academy of Sciences, Beijing 100049, China

Received 2012 April 22; accepted 2012 May 29

Abstract We report on the properties of strong pulses from PSR B0656+14 by analyzing the data obtained using the Urumqi 25-m radio telescope at 1540 MHz from August 2007 to September 2010. In 44 h of observational data, a total of 67 pulses with signal-to-noise ratios above a 5σ threshold were detected. The peak flux densities of these pulses are 58 to 194 times that of the average profile, and their pulse energies are 3 to 68 times that of the average pulse. These pulses are clustered around phases about 5° ahead of the peak of the average profile. Compared with the width of the average profile, they are relatively narrow, with the full widths at half-maximum ranging from 0.28° to 1.78° . The distribution of pulse-energies follows a lognormal distribution. These sporadic strong pulses detected from PSR B0656+14 have different characteristics from both typical giant pulses and its regular pulses.

Key words: stars: neutron-pulsars — pulsars: individual (B0656+14)

1 INTRODUCTION

PSR B0656+14 was firstly detected in the radio band by Manchester et al. (1978). The pulsar has a period of 0.3849 s. The average pulse flux density of this pulsar is 3.7 mJy at 1.4 GHz (Lorimer et al. 1995), and its dispersion measure (DM) is $13.977 \text{ pc cm}^{-3}$. The distance inferred from the DM using the free electron density model of Cordes & Lazio (2002) is $\approx 0.76 \text{ kpc}$, with a typical error of 20%, while interpretation of X-ray data gives $d = 0.2 - 0.5 \text{ kpc}$. The average profile of the pulsar presents three components, and the radiation of the main pulse component is almost completely linearly polarized, but two weak components, leading and following the main one, show low-polarization, and are more apparent at low frequencies (Gould & Lyne 1998; Weisberg et al. 2004; Hankins & Rankin 2010). PSR B0656+14 is an interesting object from which the pulsed emission has been detected in the radio, optical, soft ultraviolet, X-ray, and gamma-ray ranges of the spectrum.

Recently, very strong individual pulses have been detected from PSR B0656+14. Kuzmin & Ershov (2006) detected 52 strong individual pulses with signal-to-noise ratios (hereafter, SNRs) above the 5σ detection threshold during approximately 4.8 h of observations at 111 MHz, and the peak flux of the brightest pulse they noted was up to 640 times that of the average pulse. Weltevrede

* Supported by the National Natural Science Foundation of China.

et al. (2006b) also detected a strong pulse from the pulsar at 327 MHz, and the highest peak flux among these strong pulses was 420 times that of the average pulse. Based on this brightest burst, Weltevrede et al. (2006a) assumed that if PSR B0656+14 were located at a suitable distance, it could have been classified as a Rotating Radio Transient.

The individual pulse intensities of most radio pulsars normally fluctuate over a range of several times that of the average pulse (Ritchings 1976; Kramer et al. 2003). However, the intensities of typical giant pulses (GPs) can exceed hundreds or even thousands of times that of regular pulses (Staelin & Reifstein 1968; Cairns 2004; Knight et al. 2005). The durations of GPs are very short with timescales down to nano-seconds (Hankins et al. 2003). Unlike the GPs, the strong pulses detected from PSR B0656+14 are broad (Weltevrede et al. 2006a,b). The essential nature of the pulsar's strong pulses needs to be investigated.

To study the prominent strong pulses of bursts from B0656+14, we have been monitoring the pulsar at a higher observing frequency of 1540 MHz since August 2007. In Section 2, the observations are described in detail. In Section 3, the data analysis procedure and the results are presented. In Section 4, we discuss the results. This work is summarized in Section 5.

2 OBSERVATIONS

The observations were carried out using the Urumqi 25-m radio telescope. The telescope has a dual-channel cryogenic receiver that receives orthogonal linear polarizations at the central observing frequency of 1540 MHz. The receiver noise temperature is less than 10 K. Each polarization channel is comprised of 128 sub-channels of bandwidth 2.5 MHz, yielding a total bandwidth of 320 MHz. The data from each sub-channel are recorded to a hard disk with 1-bit sampling at 0.25 ms intervals for subsequent off-line processing (Wang et al. 2001). The minimum detected flux density of 4.8 Jy at the 5σ threshold is given by

$$S_{\min} = \frac{2\alpha\beta kT_{\text{sys}}}{\eta A \sqrt{n_p \tau \Delta f}}, \quad (1)$$

where $\alpha = 5$ is the SNR, $\beta = \sqrt{\pi/2}$ is a loss factor due to one-bit digitization, k is the Boltzmann constant, $T_{\text{sys}} = T_{\text{rec}} + T_{\text{spl}} + T_{\text{sky}} \sim 32$ K (in which T_{rec} , T_{spl} , and T_{sky} are the receiver, spillover and sky noise temperatures, respectively), $\eta \approx 57\%$ is the telescope efficiency at 1540 MHz, $A = 490.87 \text{ m}^2$ is the telescope area, $n_p = 2$ is the number of polarization channels, $\tau = 0.25$ ms is the sampling interval, and $\Delta f = 320$ MHz is the total observing bandwidth of each channel (Esamdin et al. 2008). The average pulse flux density of PSR B0656+14 is 3.7 mJy at 1.4 GHz, so we should note that only very strong single pulses (if they exist) from the pulsar can be detected using the Urumqi 25-m radio telescope.

From August 2007 to September 2010, 44 hours of data were collected in 23 observing sessions. For each observation, the sampling interval was 0.25 ms, and the timespan lasted about 2 h.

3 DATA ANALYSIS AND RESULTS

3.1 Data Analysis

Since the group velocities of radio waves in the propagation medium depend on frequency, the pulsed radiation of radio emission from a pulsar becomes dispersed in the ionized plasma of the interstellar medium. Therefore, the high frequency components of the radio pulse arrive earlier than those at lower frequencies. These dispersion delays must be removed in order to obtain the real profile of a pulse. The time difference Δt (in ms) between the arrivals of two components at different frequencies is given by

$$\Delta t = 4.1488 \times \text{DM} \times \left(\frac{1}{f_1^2} - \frac{1}{f_h^2} \right), \quad (2)$$

in which DM is the dispersion measure in pc cm^{-3} , and f_l and f_h (in GHz) represent the values of the lower and higher frequencies, respectively. The time delay was calculated using this equation for each of the 128 observing channels of each polarization.

The data were de-dispersed by delaying successive channels relative to the nominal dispersion measure of the pulsar, $\text{DM} = 13.977 \text{ pc cm}^{-3}$. Then, all pulsed signals above the 5σ threshold were identified as the candidates of pulses. And then, in order to distinguish instrumental signals or impulsive terrestrial Radio Frequency Interference (RFI) from the strong pulses of PSR B0656+14, the de-dispersion procedure was applied from 0.977 to 30.977 pc cm^{-3} at intervals of 0.1 pc cm^{-3} . For details of the pulse-identification process, see Esamdin et al. (2008).

A total of 67 pulses were detected through the process mentioned above from 44 hours of data. Approximately 1 pulse was detected for every 6100 rotation periods of the pulsar. Phases of these individual pulses were calculated by

$$\Phi(t) = \Phi_0 + \nu(t - t_0) + \frac{1}{2}\dot{\nu}(t - t_0)^2 + \frac{1}{6}\ddot{\nu}(t - t_0)^3, \quad (3)$$

where $\Phi_0 = 83.23^\circ$ is the rotational phase at time t_0 (MJD 54934.3278), t is the observation time of the strong individual pulse, $\nu = 2.59796969281 \text{ Hz}$ is the rotation frequency of the pulsar, $\dot{\nu} = -3.709653 \times 10^{-13} \text{ s}^{-2}$ is the derivative of frequency, $\ddot{\nu} = 1.03 \times 10^{-24} \text{ s}^{-3}$ is the second derivative of frequency, and all quantities were defined at time t_0 which was obtained by an observation with an average profile of the highest SNR on 2009 April 13.

We investigated the phases of these single pulses by comparing the residuals of the pulse arrival times obtained using the single-pulse timing method. In order to compare the phases of the single pulses with that of the average pulse profile of this pulsar, the average pulse profile of each observation was generated by folding all successive individual pulses. Then, we matched the profiles that were in phase during the complete period of observation with the profile of the highest SNR obtained on 2009 April 13.

3.2 Results

The bottom panel of Figure 1 shows the normalized peak flux densities of the pulses versus their phases (i.e. the peak flux densities F_i of these pulses are normalized to the average of the peak flux densities $\langle F_p \rangle$). The peak flux densities of the pulses are above $58 \langle F_p \rangle$, and the brightest burst is about 194 times stronger than the average pulse. These pulses are indeed very strong compared with the average pulse of the pulsar. We also compare the phases of the strong pulses with the radiation window of the pulsar by plotting the average profile (dotted line) in the bottom panel of Figure 1, and where the peak of the average profile is set at a phase of 0° . The top panel of Figure 1 presents the histogram of the phases of the detected strong pulses. The strong pulses are distributed over a broad pulse window with the phase range from -30° to 11.5° . However, most of the pulses are clustered around a phase about 5° earlier than the phase of the average-profile peak.

Figure 2 shows the normalized peak-flux densities versus the full widths at half maximum (FWHM, W_{50}) of the 67 detected pulses. The W_{50} of these pulses range from 0.28 to 1.78° . Most of the strong pulses are single-peaked. Compared with the width of the average profile, these pulses are narrow.

Figure 3 presents the pulse-energy distribution of the 67 strong pulses. The pulse energies are normalized to that of the average profile. Here, the peak of each pulse was arranged to lie in the 512th of 1024 bins. A set of 300 consecutive bins, from the 362nd to the 661st, was selected as the pulse window, and 300 consecutive bins of the remaining bins, which were far away from the peak of each pulse, were used to remove a baseline from the pulse window. Then, the energies of each pulse, E , were obtained. The energies of the average profiles ($\langle E \rangle$) were obtained in the same way. The energies of all single pulses were normalized to the average pulse-energy ($\langle E \rangle$) of the pulsar.

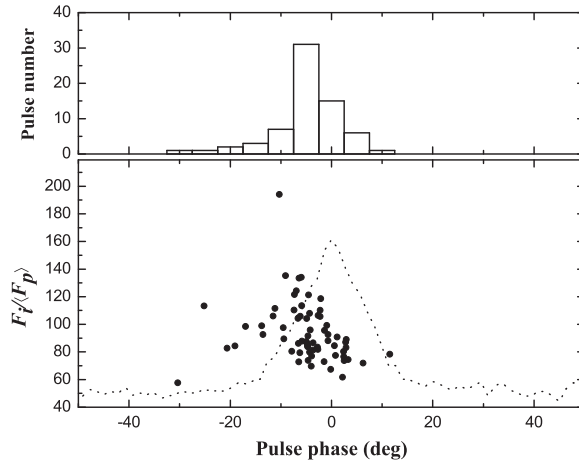


Fig. 1 A histogram showing the phase distribution of the detected strong pulses (*top panel*) and the normalized peak flux densities versus phases of the strong pulses (*bottom panel*). In order to compare single pulse phases with the phase of the average profile, the average profile is presented by a dotted line in the bottom panel (the y -axis label of the average profile is in an arbitrary unit).

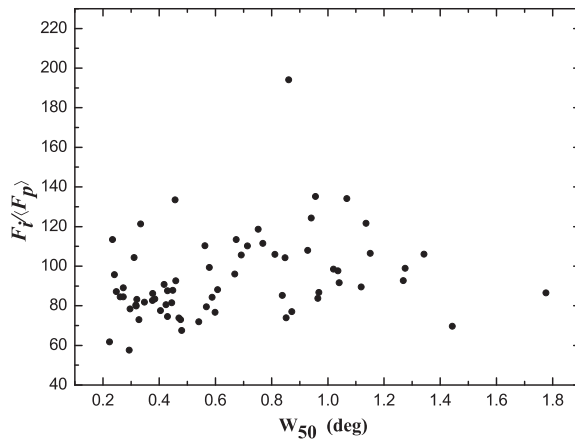


Fig. 2 The normalized peak flux densities versus W_{50} of the 67 strong pulses detected from PSR B0656+14 at 1540 MHz.

The histogram of pulse energy is presented in Figure 3. The energies of the pulses range from $3\langle E \rangle$ to $68\langle E \rangle$.

As shown in Figure 3, the pulse-energy distribution is probably best represented by a lognormal distribution. The equation is given by

$$P_{\text{lognormal}}(E) = P_0 + \frac{A\langle E \rangle}{\sqrt{2\pi\sigma E}} \exp \left[- \left(\ln \frac{E}{\langle E \rangle} - \mu \right)^2 / (2\sigma^2) \right], \quad (4)$$

where our best fitting parameters are $P_0 = 0.62$, $A = 317.35$, $\mu = 2.16$ and $\sigma = 0.66$.

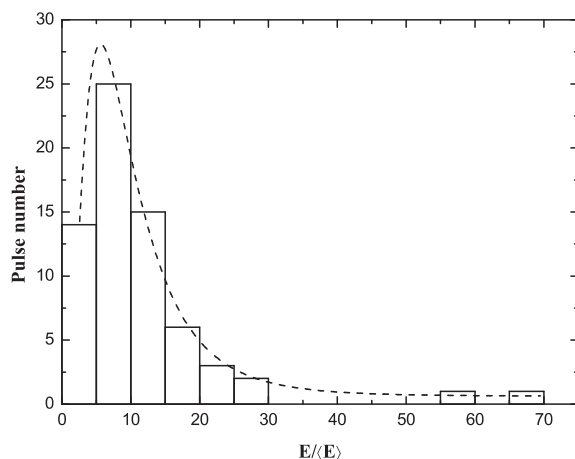


Fig. 3 The pulse-energy distribution of the strong pulses detected in this work. The energies are normalized to the average pulse-energy ($\langle E \rangle$) of the pulsar. The dashed curve shows a lognormal fitting to the pulse-energy distribution.

4 DISCUSSION

By analyzing observational data at 111 MHz, Kuzmin & Ershov (2006) suggested that PSR B0656+14 belongs to a group of pulsars which emit giant pulses. They noted that the pulse-energy distribution follows a power law, and that those so-called giant pulses are clustered in a narrow pulse-longitude range (Kuzmin & Ershov 2006). The typical GPs were very narrow with timescales down to nanoseconds (Hankins et al. 2003; Knight et al. 2006), and their energy could easily exceed 10 times that of the average pulse. The GP phenomenon has only been detected in two young pulsars: the Crab pulsar and PSR B0540–69 (Staelin & Reifenstein 1968; Wolszczan et al. 1984), and in five millisecond pulsars (Romani & Johnston 2001; Johnston & Romani 2003; Joshi et al. 2004; Knight et al. 2005). Although these seven pulsars have very different rotation rates, all of them have strong magnetic fields at the light cylinder, $B_{LC} > 10^5$ G. It is suggested that GPs are inherent in pulsars with extremely strong magnetic fields at the light cylinder, and that they may originate near the region around the light cylinder (Lyutikov 2007).

The magnetic field of PSR B0656+14 at the light cylinder is 766 G, which is much lower than those of the classical GP emitters ($B_{LC} > 10^5$ G). The pulse energy of most pulses we detected exceeded $10 \langle E \rangle$, which is within the range of GP energies. However, these pulses are much broader than GPs, and are distributed over a wide pulse window. Furthermore, the strong pulses from PSR B0656+14 showed a lognormal pulse-energy distribution rather than a power law of GPs. However, due to the small number of strong pulses we observed, more data are required to confirm whether the distribution is intrinsically lognormal. Our results are similar to those presented by Weltevrede et al. (2006a,b). The sporadic strong pulses are so strong that they can hardly be explained by the high end of intrinsic intensity-modulation of their regular pulses, or by the interstellar scintillation considering the timescales of the bursts of pulses and the broad observing band.

While the intensities of regular single pulses from PSR B0656+14 can vary at random with values reaching several times the average, they are far below the intensities of observed strong pulses. Furthermore, the phase distribution of the strong pulses cluster around 5° earlier in longitude than the peak of the average profile of the pulsar. These may suggest a difference in origin between the strong pulses detected from the pulsar and its regular pulses. It may be possible that the sporadic strong pulses and the regular pulses of PSR B0656+14 represent two different emission modes, i.e.

the strong and weak (normal) modes, with the duration of the strong mode being less than one pulse period. Further studies of the pulsar are necessary.

5 SUMMARY AND CONCLUSIONS

We have presented an analysis of the 67 strong pulses detected from PSR B0656+14 at 1540 MHz using the Urumqi 25-m radio telescope. The peak flux densities of these pulses are 58 to 194 times that of the average pulse, and their pulse energies are from 3 to 68 times that of the average pulse. The durations of the strong pulses are relatively short, ranging from 0.28° to 1.78° . By covering about 41.5° of the phase range, the strong pulses occurred over a broad range of the emission window. However, they are mainly clustered around the phase about 5° earlier than that of the average-profile peak. The sporadic strong pulses detected from PSR B0656+14 have different characteristics from the typical GPs emitted by some other pulsars, and may also be different from its regular pulses.

Acknowledgements We thank the referee for helpful comments on the paper. This work was funded by the National Natural Science Foundation of China (Grant No. 10973026).

References

- Cairns, I. H. 2004, *ApJ*, 610, 948
 Cordes, J. M., & Lazio, T. J. W. 2002, arXiv:astro-ph/0207156
 Esamdin, A., Zhao, C. S., Yan, Y., et al. 2008, *MNRAS*, 389, 1399
 Gould, D. M., & Lyne, A. G. 1998, *MNRAS*, 301, 235
 Hankins, T. H., Kern, J. S., Weatherall, J. C., & Eilek, J. A. 2003, *Nature*, 422, 141
 Hankins, T. H., & Rankin, J. M. 2010, *AJ*, 139, 168
 Johnston, S., & Romani, R. W. 2003, *ApJ*, 590, L95
 Joshi, B. C., Kramer, M., Lyne, A. G., McLaughlin, M. A., & Stairs, I. H. 2004, in *IAU Symposium 218, Young Neutron Stars and Their Environments*, eds. F. Camilo, & B. M. Gaensler, 319
 Knight, H. S., Bailes, M., Manchester, R. N., & Ord, S. M. 2005, *ApJ*, 625, 951
 Knight, H. S., Bailes, M., Manchester, R. N., Ord, S. M., & Jacoby, B. A. 2006, *ApJ*, 640, 941
 Kramer, M., Karastergiou, A., Gupta, Y., et al. 2003, *A&A*, 407, 655
 Kuzmin, A. D., & Ershov, A. A. 2006, *Astronomy Letters*, 32, 583
 Lorimer, D. R., Yates, J. A., Lyne, A. G., & Gould, D. M. 1995, *MNRAS*, 273, 411
 Lyutikov, M. 2007, *MNRAS*, 381, 1190
 Manchester, R. N., Lyne, A. G., Taylor, J. H., et al. 1978, *MNRAS*, 185, 409
 Ritchings, R. T. 1976, *MNRAS*, 176, 249
 Romani, R. W., & Johnston, S. 2001, *ApJ*, 557, L93
 Staelin, D. H., & Reifenstein, E. C., III 1968, *Science*, 162, 1481
 Wang, N., Manchester, R. N., Zhang, J., et al. 2001, *MNRAS*, 328, 855
 Weisberg, J. M., Cordes, J. M., Kuan, B., et al. 2004, *ApJS*, 150, 317
 Weltevrede, P., Stappers, B. W., Rankin, J. M., & Wright, G. A. E. 2006a, *ApJ*, 645, L149
 Weltevrede, P., Wright, G. A. E., Stappers, B. W., & Rankin, J. M. 2006b, *A&A*, 458, 269
 Wolszczan, A., Cordes, J., & Stinebring, D. 1984, in *Birth and Evolution of Neutron Stars: Issues Raised by Millisecond Pulsars*, eds. S. P. Reynolds, & D. R. Stinebring, 63